Analysis of a Steel-Concrete Composite Plate resting on Axial Bars using the Finite Element Method

Nguyen Ngoc Long
University of Transport and Communications, Vietnam
nguyenngoclong@utc.edu.vn

Nguyen Xuan Tung
University of Transport and Communications, Vietnam
ngxuantung@utc.edu.vn (corresponding author)

Received: 12 May 2023 | Revised: 13 June 2023 | Accepted: 18 June 2023

 DOI: https://doi.org/10.48084/etasr.6036

ABSTRACT

This study applied finite element analysis to a steel-concrete composite plate resting on the axial bar, using a four-node quadrilateral finite element for a steel-concrete composite plate combined with a truss element. Plate displacements and deformations were used to formulate the finite element method based on the first-order plate theory, also known as the Mindlin plate theory. The finite element analysis to combine steel-concrete composite plates and axial bars was implemented in MATLAB. Numerical examples were used in detail, showing a very small difference between the current study and the SAP2000 results.

Keywords-axial bar; truss; finite element method; bending plate

I. INTRODUCTION

Many researchers and companies have studied and developed various types of composite structures that combine concrete and steel, such as reinforced concrete beams, steel-concrete composite beams [1-2], reinforced concrete slabs, and steel-concrete composite slabs [3]. A steel-concrete composite slab can be used to increase the stiffness and reduce the thickness of the slab. In some cases, steel-concrete composite slabs rest on bar members, such as trusses, forming a complex structure consisting of the slab and the axial bar. Such a structure can satisfy both the strength and architectural design requirements.

Many studies investigated the characteristics of composite materials and proposed calculation methods for slab and shell structures. In [4], the uniform thickness of a plate was studied with the 4-node finite element method. In [5], the calculation of composite panels was investigated by considering the viscosity of the material using the finite element method. In [6], the element-free Galerkin method was used to calculate a plate with elastic connections at the edge. In [7], ANSYS 10.0 was used to calculate the nonlinear oscillations of composite panels subjected to impulses. In [8], the critical loads of a cracked nanoplate with variable thickness were studied with the finite element method. In [9], the finite element method was used for the stability calculation of inclined composite slabs with cuts. An experimental study on the shear resistance of fire-resistant reinforced concrete slabs was conducted in [10]. In [11], an analysis of the effect of the shape of the impact tip on damage was carried out during a low-speed impact on the composite panel using a three-dimensional finite element model. In [12], an arbitrary quadrangular finite element was considered for the bending of a plate using the piecewise constant approximation of moments. In [13], the static bending of rectangular plates resting on a non-uniform foundation was solved using the Ritz method. In [14], the dynamic behavior of a buried fiber-reinforced concrete slab under blast load was investigated using the Femap finite element software. In [15], the upper bound limit loads of plate bending were computed using a conforming Hsieh-Clough-Tocher element. In [16], the dynamic displacement of functionally graded plates lying on the viscoelastic foundation was solved using the analytical method. In [17], the transient response of a reinforced concrete plate resting on an elastic foundation subjected to dynamic load was calculated using the state-space method. In [18-19], the natural frequency of a cracked plate with variable thickness was calculated using the finite element method combined with phase field theory. The dynamic responses of non-isothermic viscoelastic-plastic reinforced plates were solved using the semi-analytical method in [20]. In [21], the shear capacity of a steel-concrete composite trussed beam was investigated using an analytical approach.

As steel concrete composite plates associated with bar structures, such as beams and trusses, are very popular in construction, it is necessary to develop programs to calculate the internal forces of the plates so that engineers can easily

access design calculations. Although there are many studies on plates, the use of the 4-node element for plates associated with axial bars is rare. Therefore, this study focused on creating a finite element model for the Mindlin plate associated with axial bars. This paper presents a numerical method for coupling the axial bars and plate structure.

II. FINITE ELEMENT EQUATION OF PLATES

This study considered a plate with the geometry shown in Figure 1.

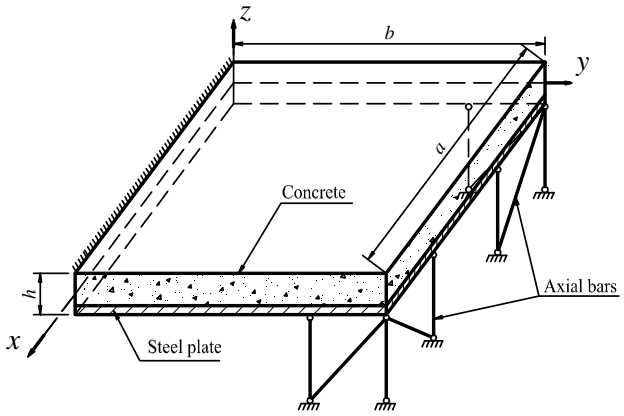

Fig. 1. The geometry of the plate.

The displacement fields at an arbitrary point (*x, y, z*) in the plate are calculated using the first shear strain theory, also known as Mindlin plate theory [22], as follows:

$$\begin{aligned} U(x,y,z) &= u(x,y) + z\psi_x(x,y) \\ V(x,y,z) &= v(x,y) + z\psi_x(x,y) \\ W(x,y,z) &= w \quad (x,y) \end{aligned} \tag{1}$$

The deformations obtained from the displacements are as follows:

$$\begin{Bmatrix} \varepsilon_{xx} \\ \varepsilon_{yy} \\ \gamma_{xy} \\ \gamma_{xz} \\ \gamma_{yz} \end{Bmatrix} = \begin{Bmatrix} \frac{\partial u}{\partial x} \\ \frac{\partial v}{\partial y} \\ \frac{\partial u}{\partial y} + \frac{\partial v}{\partial x} \\ \frac{\partial u}{\partial z} + \frac{\partial w}{\partial x} \\ \frac{\partial v}{\partial z} + \frac{\partial w}{\partial y} \end{Bmatrix} \tag{2}$$

or:

$$\varepsilon = \begin{Bmatrix} \varepsilon_{xx} \\ \varepsilon_{yy} \\ \gamma_{xy} \end{Bmatrix} = \begin{Bmatrix} \varepsilon_{xx}^{m} \\ \varepsilon_{yy}^{m} \\ \gamma_{xy}^{m} \end{Bmatrix} + z \begin{Bmatrix} \varepsilon_{xx}^{f} \\ \varepsilon_{yy}^{f} \\ \gamma_{xy}^{f} \end{Bmatrix}$$

$$\gamma = \begin{Bmatrix} \gamma_{xz} \\ \gamma_{yz} \end{Bmatrix} = \begin{Bmatrix} \gamma_{xz}^{(0)} \\ \gamma_{yz}^{(0)} \end{Bmatrix} \tag{3}$$

The *u*, *v*, *w* displacement of the element was approximated over the generalized displacements at the node using the form [23-24]:

$$\begin{aligned} U &= \sum_{i=1}^{4} N_i u_I \,; v = \sum_{i=1}^{4} N_i v_I \,; w = \sum_{i=1}^{4} N_i w_i \\ \psi_x &= \sum_{i=1}^{4} N_i \theta_i \,; \psi_y = \sum_{i=1}^{4} N_i \theta_i \end{aligned} \tag{4}$$

where the form functions of the 4-node quadrilateral element are:

$$\begin{aligned} N_1(\xi,\eta) &= l_1(\xi) l_1(\eta) = \tfrac{1}{4}(1-\xi)(1-\eta) \\ N_2(\xi,\eta) &= l_2(\xi) l_1(\eta) = \tfrac{1}{4}(1+\xi)(1-\eta) \\ N_3(\xi,\eta) &= l_2(\xi) l_2(\eta) = \tfrac{1}{4}(1+\xi)(1+\eta) \\ N_4(\xi,\eta) &= l_1(\xi) l_2(\eta) = \tfrac{1}{4}(1-\xi)(1+\eta) \end{aligned} \tag{5}$$

Substituting the approximations of (4) into the strain expression (3), the deformation matrix *B* [22], comprised of the following components, is obtained:

- Corresponding to the membrane deformation part:

$$B_m^{(e)} = \begin{bmatrix} \frac{\partial N}{\partial x} & 0 & 0 & 0 & 0 \\ 0 & \frac{\partial N}{\partial y} & 0 & 0 & 0 \\ \frac{\partial N}{\partial y} & \frac{\partial N}{\partial x} & 0 & 0 & 0 \end{bmatrix} \tag{6}$$

- Corresponding to the bending deformation part:

$$B_f^{(e)} = \begin{bmatrix} 0 & 0 & 0 & \frac{\partial N}{\partial x} & 0 \\ 0 & 0 & 0 & 0 & \frac{\partial N}{\partial y} \\ 0 & 0 & 0 & \frac{\partial N}{\partial y} & \frac{\partial N}{\partial x} \end{bmatrix} \tag{7}$$

- Corresponding to the shear deformation part:

$$B_c^{(e)} = \begin{bmatrix} 0 & 0 & \frac{\partial N}{\partial x} & N & 0 \\ 0 & 0 & \frac{\partial N}{\partial y} & 0 & N \end{bmatrix} \tag{8}$$

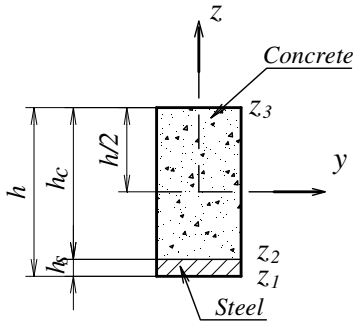

Fig. 2. Cross section of the plate.

The stiffness matrix of the finite elements of the plate is:

$$K_{plate}^{(e)} = K_{mm}^{(e)} + K_{mf}^{(e)} + K_{fm}^{(e)} + K_{ff}^{(e)} + K_{cc}^{(e)} \tag{9}$$

where:

$$K_{mm}^{(e)} = \underbrace{\int_A B_m^T D_k B_m (z_{k+1} - z_k)\, dA}_{Steel} + \underbrace{\int_A B_m^T D_k B_m (z_{k+1} - z_k)\, dA}_{Concrete} \quad (10)$$

$$K_{mf}^{(e)} = \underbrace{\frac{1}{2}\int_A B_m^T D_k B_f (z_{k+1}^2 - z_k^2)\, dA}_{Steel} + \underbrace{\frac{1}{2}\int_A B_m^T D_k B_f (z_{k+1}^2 - z_k^2)\, dA}_{Concrete} \quad (11)$$

$$K_{fm}^{(e)} = \underbrace{\frac{1}{2}\int_A B_f^T D_k B_m (z_{k+1}^2 - z_k^2)\, dA}_{Steel} + \underbrace{\frac{1}{2}\int_A B_f^T D_k B_m (z_{k+1}^2 - z_k^2)\, dA}_{Concrete} \quad (12)$$

$$K_{ff}^{(e)} = \underbrace{\frac{1}{3}\int_A B_f^T D_k B_f (z_{k+1}^3 - z_k^3)\, dA}_{Steel} + \underbrace{\frac{1}{3}\int_A B_f^T D_k B_f (z_{k+1}^3 - z_k^3)\, dA}_{Concrete} \quad (13)$$

$$K_{cc}^{(e)} = \underbrace{\int_A B_c^T D_c B_c (z_{k+1}^2 - z_k^2)\, dA}_{Steel} + \underbrace{\int_A B_s^T D_c B_c (z_{k+1}^2 - z_k^2)\, dA}_{Concrete} \quad (14)$$

where the subscripts *m*, *f*, and *c* in (9)-(12) correspond to the membrane, bending, and shear deformation part, respectively. The stiffness matrix of the system includes the stiffness matrix of the plate and the axial bar:

$$K = K_{Plate} + K_{Axial-Bar} \quad (15)$$

III. NUMERICAL EXAMPLES

Consider a rectangular steel concrete composite plate that rests on simply supported or axial bars, as shown in Figures 3 and 4. The plate is rectangular with dimensions: a = 3 m, b = 3 m, thickness in a range of 8-15 cm, and 10 mm thickness of the steel plate. The steel concrete composite plate was subjected to a uniform load of q_0 = 8 kN/m^2. Table I shows the properties of the material.

TABLE I. MATERIAL PROPERTIES

Materials	Elastic modulus (GPa)	Poisson's ratio
Concrete	30	0.25
Steel	200	0.3

A. Example 1

To verify the accuracy of the present approach, the steel-concrete composite plate rested on axial bars, and two cases were considered to compare with the SAP2000 results:

- Case 1: The plate is supported on 2 simple supports and 2 edges of the plate rest on tension bars, as shown in Figure 3.
- Case 2: The plate is free on all edges and rests on tension bars, as shown in Figure 4.

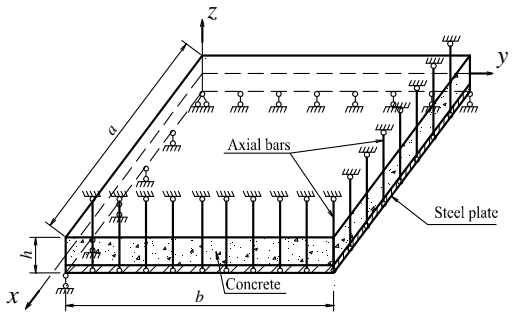

Fig. 3. Plate with 2 edges simply supported and axial bars.

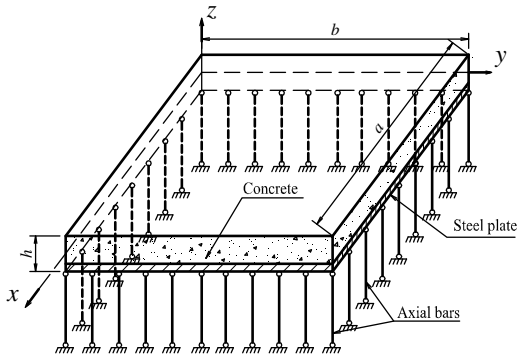

Fig. 4. Plate rest on axial bars on all edges.

Finite element analysis was carried out on steel-concrete composite plates with a thickness of 8 cm, meshed in 10×10. Figure 5 shows the displacement of the plate corresponding to cases 1 and 2.

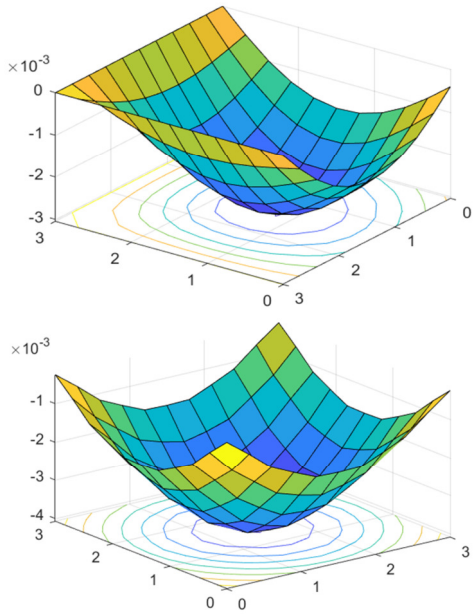

Fig. 5. Displacement of plate: (a) case 1 and (b) case 2.

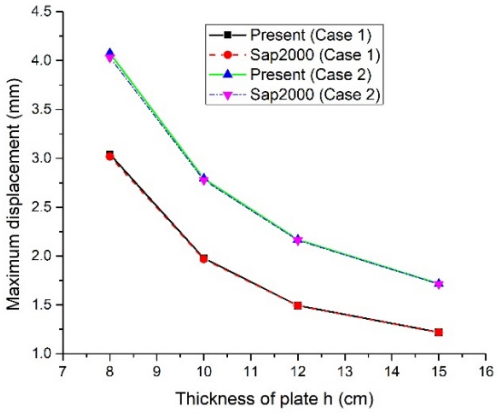

Fig. 6. The maximum displacement of the plate.

Figure 6 and Table II show the maximum plate displacement calculated in the present study and using SAP2000, showing that there is a good agreement between the two methods. Figure 7 shows that the maximum displacement decreases rapidly as the thickness of the plate increases, even though the thickness of the steel plate remains constant.

TABLE II. MAXIMUM DISPLACEMENT

Plate thickness *h* (cm)		**Maximum displacement (mm)**		
		Present	**Sap2000**	**Error (%)**
Case 1	8	3.042	3.017	0.83
	10	1.978	1.968	0.51
	12	1.493	1.491	0.13
	15	1.220	1.219	0.08
Case 2	8	4.075	4.033	1.04
	10	2.793	2.778	0.54
	12	2.168	2.161	0.32
	15	1.716	1.714	0.12

B. Example 2

The steel concrete composite plate was free at three edges and rested on tension bars, as shown in Figure 4. Figures 7 and 9 clearly show the influence of foundation stiffness on the displacement distribution of the plate. When the plate is thinner, the stiffness is lower and the displacement is like simply supported plates. In thick plates, the stiffness is high and the deflection is like an inclined surface to the side of the axial bars.

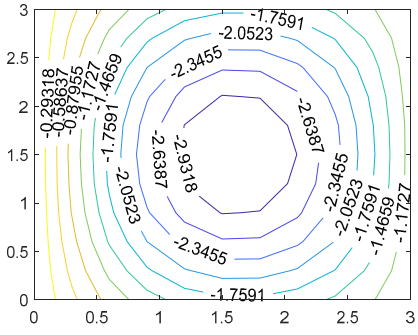

Fig. 7. Maximum displacement of the plate (h=8cm)

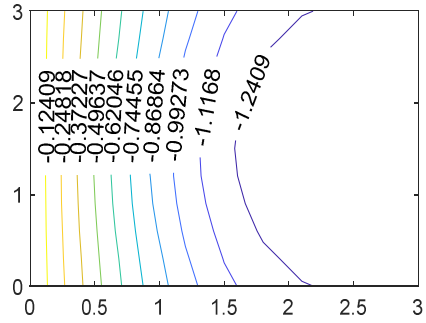

Fig. 8. Maximum displacement of the plate (h=15cm).

IV. CONCLUSIONS

This study presented the application of the finite element method on steel concrete composite plates with axial bar connections at the edges. Finite element formulas for steel-concrete composite plates were established using the Mindlin plate theory and the four-node quadrilateral element. Using these formulas, an algorithm was developed and coded in Matlab. The numerical example results demonstrated the influence of the thickness of the plate on its displacements. The maximum displacement of the plate decreased rapidly as its thickness increased. The distribution of the displacement also changed depending on its thickness. The proposed method and its results are very useful for engineers in the study and design of steel concrete composite plates associated with axial bars.

ACKNOWLEDGEMENT

This research is funded by Vietnam Ministry of Education and Training under grant number B2022-GHA-04

REFERENCES

[1] T. P. Ba and A. L. Van, "Structural analysis of steel-concrete composite beam bridges utilizing the shear connection model," *Transport and Communications Science Journal*, vol. 72, no. 7, pp. 811–823, 2021, https://doi.org/10.47869/tcsj.72.7.4.

[2] H. D. Ta, K. T. Nguyen, T. D. Ngoc, H. T. Do, T. X. Nguyen, and D. D. Nguyen, "Approximation solution for steel concrete beam accounting high-order shear deformation using trigonometric-series," *Journal of Materials and Engineering Structures « JMES »*, vol. 9, no. 4, pp. 599–605, Dec. 2022.

[3] H. Kuhair, S. Hama, and K. Aziz, "Long–term behavior of composite steel plate-concrete slabs incorporating waste plastic fibers," *Magazine of Civil Engineering*, vol. 109, no. 1, pp. 10904–10904, 2022, https://doi.org/10.34910/MCE.109.4.

[4] A. Ibrahimbegović, "Quadrilateral finite elements for analysis of thick and thin plates," *Computer Methods in Applied Mechanics and Engineering*, vol. 110, no. 3, pp. 195–209, Dec. 1993, https://doi.org/10.1016/0045-7825(93)90160-Y.

[5] R. B. Rikards, A. K. Chate, and A. V. Korjakin, "Damping analysis of laminated composite plates by finite-element method," *Mechanics of Composite Materials*, vol. 30, no. 1, pp. 68–78, Jan. 1994, https://doi.org/10.1007/BF00612736.

[6] Y. Wang, Z. Wang, and M. Ruan, "Element-free Galerkin method for free vibration of rectangular plates with interior elastic point supports and elastically restrained edges," *Journal of Shanghai University (English Edition)*, vol. 14, no. 3, pp. 187–195, Jun. 2010, https://doi.org/10.1007/s11741-010-0628-2.

[7] Z. Kazanci, "Nonlinear transient response of a laminated composite plate under time-dependent pulses," in *2009 4th International Conference on*

Recent Advances in Space Technologies, Istanbul, Turkey, Jun. 2009, pp. 125–130, https://doi.org/10.1109/RAST.2009.5158181.

[8] D. D. Hong, D. V. Thom, and P. P. Minh, "Buckling analysis of variable thickness cracked nanoplates considerting the flexoelectric effect," *Transport and Communications Science Journal*, vol. 73, no. 5, pp. 470–485, 2022, https://doi.org/10.47869/tcsj.73.5.3.

[9] S. Y. Lee, "Finite element dynamic stability analysis of laminated composite skew plates containing cutouts based on HSDT," *Composites Science and Technology*, vol. 70, no. 8, pp. 1249–1257, Aug. 2010, https://doi.org/10.1016/j.compscitech.2010.03.013.

[10] A. N. Dalaf and S. D. Mohammed, "The Impact of Hybrid Fibers on Punching Shear Strength of Concrete Flat Plates Exposed to Fire," *Engineering, Technology & Applied Science Research*, vol. 11, no. 4, pp. 7452–7457, Aug. 2021, https://doi.org/10.48084/etasr.4314.

[11] M. Rabouh, K. Guerraiche, K. Zouggar, and D. Guerraiche, "Bridging the Effect of the Impactor Head Shape to the Induced Damage during Impact at Low Velocity for Composite Laminates," *Engineering, Technology & Applied Science Research*, vol. 13, no. 1, pp. 9973–9984, Feb. 2023, https://doi.org/10.48084/etasr.5446.

[12] Y. Tyukalov, "Arbitrary quadrangular finite element for plates with shear deformations," *Magazine of Civil Engineering*, vol. 107, no. 7, pp. 10707–10707, 2021, https://doi.org/10.34910/MCE.107.7.

[13] T. D. Hien and B. T. Quang, "Analysis of isotropic rectangular plate resting on non-uniform elastic foundation using Ritz approach," *Materials Today: Proceedings*, vol. 19, pp. 158–160, Jan. 2019, https://doi.org/10.1016/j.matpr.2019.06.631.

[14] A. Alekseytsev and S. Sazonova, "Numerical analysis of the buried fiber concrete slabs dynamics under blast loads," *Magazine of Civil Engineering*, vol. 117, no. 1, pp. 11703–11703, 2023, https://doi.org/10.34910/MCE.117.3.

[15] T. D. Tran and P. H. V. Nguyen, "Computation of Limit Loads for Bending Plates," *Engineering, Technology & Applied Science Research*, vol. 13, no. 2, pp. 10466–10470, Apr. 2023, https://doi.org/10.48084/etasr.5671.

[16] D. T. Thuy, L. N. Ngoc, D. N. Tien, and H. V. Thanh, "An Analytical Solution for the Dynamics of a Functionally Graded Plate resting on Viscoelastic Foundation," *Engineering, Technology & Applied Science Research*, vol. 13, no. 1, pp. 9926–9931, Feb. 2023, https://doi.org/10.48084/etasr.5420.

[17] N. T. Hiep, "Dynamic analysis of reinforced concrete plate resting on elastic foundation using state space method and refined plate theory," *Civil and Environmental Science Journal (CIVENSE)*, vol. 6, no. 1, pp. 84–89, Apr. 2023, https://doi.org/10.21776/ub.civense.2023.00601.10.

[18] P. Pham Minh, "Using phase field and third-order shear deformation theory to study the effect of cracks on free vibration of rectangular plates with varying thickness," *Transport and Communications Science Journal*, vol. 71, pp. 853–867, Sep. 2020, https://doi.org/10.47869/tcsj.71.7.10.

[19] P. P. Minh, "Analysis free vibration of the functionally grade material cracked plates with varying thickness using the Phase-field theory," *Transport and Communications Science Journal*, vol. 70, no. 2, pp. 122–131, 2019, https://doi.org/10.25073/tcsj.70.2.35.

[20] A. P. Yankovskii, "Modeling of Nonisothermic Viscoelastic–Plastic Behavior of Flexible Reinforced Plates," *Journal of Applied Mechanics and Technical Physics*, vol. 63, no. 7, pp. 1243–1263, Dec. 2022, https://doi.org/10.1134/S0021894422070173.

[21] G. Campione, P. Colajanni, and A. Monaco, "Analytical evaluation of steel–concrete composite trussed beam shear capacity," *Materials and Structures*, vol. 49, no. 8, pp. 3159–3176, Aug. 2016, https://doi.org/10.1617/s11527-015-0711-6.

[22] A. J. M. Ferreira and N. Fantuzzi, *MATLAB Codes for Finite Element Analysis: Solids and Structures*, vol. 157. Cham, Switzerland: Springer International Publishing, 2020.

[23] N. Reddy, *Introduction to the Finite Element Method*, 4th Ed. New York, NY, USA: McGraw-Hill Education, 2019.

[24] S. S. Rao, *The Finite Element Method in Engineering*. Oxford, UK: Butterworth-Heinemann, 2017.